Three New vic-Dioxime Ligands: Synthesis, Characterization, Spectroscopy, and Redox Properties of Their Mononuclear Nickel(II) Complexes

Ahmet Kilic[1], Esref Tas[1], Bahattin Gumgum[2], and Ismail Yilmaz[3]

[1]*Department of Chemistry, Harran University, Sanliurfa, Osmanbey, Turkey*

[2]*Department of Chemistry, Dicle University, Diyarbakir, Turkey*

[3]*Department of Chemistry, Technical University of Istanbul, Istanbul, Maslak, Turkey*

ABSTRACT: *Nickel(II) complexes with three new vic-dioxime reagents, N-(ethyl-4-amino-1-piperidine carboxylate)phenylglyoxime (L_1H_2), N-(ethyl-4-amino-1-piperidine carboxylate)glyoxime (L_2H_2) and N,N'-bis(ethyl-4-amino-1-piperidine carboxylate)glyoxime (L_3H_2), have been prepared. Mononuclear nickel(II) complexes with a metal/ligand ratio of 1:2 were prepared using Ni(II) salt. All these nickel(II) complexes are nonelectrolytes as shown by their molar conductivities (Λ_M) in DMF solution at 10^{-3} M concentration. The ligands are soluble in common solvents such as DMSO, DMF, $CHCl_3$, and C_2H_5OH. The ligands and their Ni(II) complexes were characterized by elemental analyses, FT-IR, UV-visible, ^{1}H NMR, ^{13}C NMR, magnetic susceptibility measurements, cyclic voltammetry, and molar conductivities (Λ_M). The cyclic voltammetric measurements show that $[Ni(L_1H)_2]$ and $[Ni(L_2H)_2]$ complexes exhibit almost similar electrochemical behavior, with two reduction and two oxidation processes based on either metals or oxime moities, while $[Ni(L_3H)_2\cdot2H_2O]$ complex displays irreversible, with one reduction and one oxidation processes based on oxime moity. This main difference could be attributed to the highly polarized $[Ni(L_3H)_2\cdot2H_2O]$ complex that has four carboxylate groups attached to piperidine on the oxime moieties.* © 2007 Wiley Periodicals, Inc. Heteroatom Chem 18:657–663, 2007; Published online in Wiley InterScience (www.interscience.wiley.com). DOI 10.1002/hc.20357

INTRODUCTION

Vicinal dioxime metal complexes, initiating an area of coordination chemistry, have been widely explored during the past century [1]. The chemistry of oxime/oximato metal complexes has been investigated since the time of first synthesis, for example, preparation of nickel(II) dimethylglyoximato and recognition of the chelate five-membered character of this complex by Chugaev [2]. Because of the presence of mildly acidic hydroxyl groups and slightly basic azomethine groups, vic-dioximes are amphoteric ligands that form corrin-type square-planar, square-pyramidal, and octahedral complexes with transition metal ions such as nickel(II) as the central atoms [3]. The exceptional stability and unique electronic properties of these complexes can be

attributed to their planar structure, which is stabilized by hydrogen bonding [4]. The reactions of amines with dichloroglyoxime, cyanogen-di-N-oxide, phenylglyoxime, and monochloroglyoxime yielded various symmetrically or unsymmetrically substituted diaminoglyoxime derivatives [5]. It is reported that 1,2-dioximes exist in the *anti-*, *amphi-*, and *syn-*geometric isomeric forms, depending on the position of O-H groups in the molecule [6]. The order of stability of these isomers varies in the order *anti-*, *amphi-*, and *syn-*configuration, respectively [7].

Herein, we present the synthesis of three new carboxylate-substituted *vic*-dioxime ligands (L_1H_2, L_2H_2, and L_3H_2), together with their nickel(II) complexes. These ligands were synthesized by the reaction of *anti*-phenylchloroglyoxime, *anti*-monochloroglyoxime, or *anti*-dichloroglyoxime with ethyl-4-amino-1-piperidine carboxylate, whereas Ni(II) complexes were obtained from these ligands and nickel(II) salts. The aim of this work was to understand the structure of newly synthesized Ni(II) complexes and electron transfer mechanism of their redox processes, as well as stability of their electrogenerated species.

EXPERIMENTAL

Materials and Methods

All reagents and solvents were reagent grade and obtained from commercial suppliers. Both *anti*-phenylchloroglyoxime [8] and *anti*-monochloroglyoxime [9,10] were synthesized as described in the literature, whereas (*E,E*)-dichloroglyoxime was prepared by a reported procedure [11,12]. Elemental analyses were carried out in the Laboratory of the Scientific and Technical Research Council of Turkey (TUBITAK). IR spectra were recorded on a Perkin Elmer Spectrum RXI FT-IR Spectrometer as KBr pellets, ^{1}H NMR and ^{13}C NMR spectra were recorded on a Bruker-Avence 400 MHz spectrometers. Magnetic susceptibilities were measured on a Sherwood Scientific Magnetic Susceptibility Balance (Model MK1) at room temperature (20°C) using Hg[Co(SCN)$_4$] as a calibrant; diamagnetic corrections were calculated from Pascal's constants [10]. UV-visible spectra were recorded on a Schimadzu 1601 PC. Molar conductivities (Λ_M) were recorded on a Inolab Terminal 740 WTW Series. An EcoChemie Autolab-12 potentiostat with the electrochemical software package GPES 4.9 (Utrecht, The Netherlands) was used for voltammetric measurements. A three-electrode system was used: a platinum wire counter electrode, an Ag/AgCl reference electrode, and a 2-mm-sized platinum disc electrode as working electrode. The working electrode was polished with 0.05-μm alumina prior to each experiment. Throughout the experiment, oxygen-free nitrogen was bubbled through the solution for 10 min. Voltammetric experiments were performed at room temperature. Electrochemical-grade tetraethylammonium perchlorate (TEAP) (0.1 mol dm^{-3}) was employed as the supporting electrolyte. The ferrocene/ferrocenium couple (Fc/Fc$^+$) was used as an internal standard.

Synthesis of L_1H_2, L_2H_2, and L_3H_2 Ligands

Ethyl-4-amino-1-piperidine carboxylate (1.72 g, 10 mmol for L_1H_2; 2.58 g, 15 mmol for L_2H_2; and 3.44 g, 20 mmol for L_3H_2, respectively) was dissolved in 40 cm^3 absolute THF. Then triethylamine (Et$_3$N) (1.52 g, 15 mmol for L_1H_2; 2.03 g, 20 mmol for L_2H_2; and 2.53 g, 25 mmol for L_3H_2, respectively) was added. The mixture was cooled to −15°C and kept at this temperature. To this solution, *anti*-phenylchloroglyoxime (1.99 g, 10 mmol), *anti*-monochloroglyoxime (1.84 g, 15 mmol), or *anti*-dichloroglyoxime (1.57 g, 10 mmol) in 20 cm^3 absolute THF was added dropwise under a N$_2$ atmosphere with continuous stirring. The addition of *anti*-phenylchloroglyoxime, *anti*-monochloroglyoxime, or *anti*-dichloroglyoxime solution was carried out during 2 h. The mixture was stirred for more than 1.5 h and then the temperature was raised to 20°C. Precipitated Et$_3$NHCl was filtered off and the filtrate was evaporated to remove THF. The oily product was dissolved in CH$_2$Cl$_2$ (15 cm^3), and *n*-hexane (150 cm^3) was added to precipitate the respective compound. This process was then repeated several times. The product was filtered and dried under vacuum. All products are soluble in CH$_2$Cl$_2$, THF, EtOH, and DMSO. The characteristic ^{13}C NMR chemical shifts (CDCl$_3$, TMS, δ ppm) for L_1H_2: C$_1$ (128.3), C$_2$ (129.5), C$_3$ (130.0), C$_4$ (130.2), C$_5$ (151.1), C$_6$ (149.0), C$_7$ (50.2), C$_8$ (33.4), C$_9$ (42.6), C$_{10}$ (156.6), C$_{11}$ (61.5), and C$_{12}$ (14.6); for L_2H_2: C$_1$ (143.8), C$_2$ (148.4), C$_3$ (50.1), C$_4$ (42,7), C$_5$ (61.9), C$_6$ (156.1), C$_7$ (33.8), and C$_8$ (14.8); and for L_3H_2: C$_1$ (148.1), C$_2$ (50.2), C$_3$ (42.3), C$_4$ (33.9). C$_5$ (154.3), C$_6$ (62.2), and C$_7$ (18.6).

Synthesis of Ni(II) Complexes

L_1H_2 (0.50 g, 1.5 mmol), L_2H_2 (0.39 g, 1.5 mmol), or L_3H_2 (0.64 g, 1.5 mmol) was dissolved in EtOH (40 cm^3). A solution of 0.75 mmol of the metal salt NiCl$_2\cdot$6H$_2$O (0.18 g) in EtOH (15 cm^3) was added dropwise under a N$_2$ atmosphere with continuous stirring. The stirred mixture was then heated to

reflux for 90 min and was maintained at this temperature. The pH of the solution was *ca*. 1.5–3.0 and was adjusted to 4.5–5.5 by the addition of a 1% NaOH solution in EtOH. After cooling to room temperature, the precipitated complexes were filtered, washed with H_2O and diethyl ether several times, and then dried at 100°C for 24 h under vacuum. The characteristic ^{13}C NMR chemical shifts were recorded (CDCl$_3$, TMS, δ ppm) for [Ni(L$_1$H)$_2$]: C$_1$ (128.8), C$_{2,3}$ (128.9), C$_4$ (130.0), C$_5$ (149.2), C$_6$ (143.6), C$_7$ (51.4), C$_8$ (33.7), C$_9$ (42.3), C$_{10}$ (155.3), C$_{11}$ (61.4), and C$_{12}$(14.6); for [Ni(L$_2$H)$_2$]: C$_1$ (150.0), C$_2$ (152.5), C$_3$ (50.9), C$_4$ (42,8), C$_5$ (61.4), C$_6$ (155.2), C$_7$ (33.1), and C$_8$(15.0).

RESULTS AND DISCUSSION

The reaction steps for the synthesis of L$_1$H$_2$, L$_2$H$_2$, and L$_3$H$_2$ and their structures are given in Scheme 1. *N*-(Ethyl-4-amino-1-piperidine carboxylate)phenylglyoxime (L$_1$H$_2$), *N*-(ethyl-4-amino-1-piperidine carboxylate)glyoxime (L$_2$H$_2$), and *N,N'*-bis(ethyl-4-amino-1-piperidine carboxylate)glyoxime (L$_3$H$_2$) were obtained by the reaction of *anti*-phenylchloroglyoxime, *anti*-monochloroglyoxime, or *anti*-dichloroglyoxime with ethyl-4-amino-1-piperidine carboxylate as shown in Scheme 1. Excess triethylamine was used to neutralize the liberated HCl in the reaction. Mononuclear Ni(II) complexes of L$_1$H$_2$, L$_2$H$_2$, and L$_3$H$_2$ ligands were prepared by a metal/ligand molar ratio of 1:2.

For the structural characterization of ligands and Ni(II) metal complexes, elemental analyses, FT-IR, UV-visible, ^{1}H NMR, and ^{13}C NMR spectra, magnetic susceptibility measurements, molar conductivity measurements, and cyclic voltammetry were used. Additional analytical data are given in Tables 1–5.

NMR Spectra

In the ^{1}H NMR spectra of L$_1$H$_2$ and L$_2$H$_2$ in CHCl$_3$-*d*$_1$, two peaks are present for the =N—OH protons
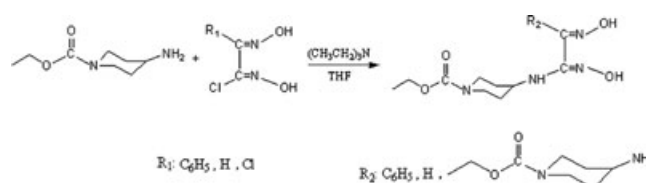
of the oxime groups. These two D$_2$O-exchangeable singlets correspond to two nonequivalent —OH protons, which also indicate the *anti*-configuration of the —OH relative to each other [5b,13,14]. The first one is assigned to the —OH proton on the phenyl side and the latter indicates the —OH proton of the amidoxime group since the effect of chemical shift on various substituents is expected to be higher on the amidoxime group [14]. In the ^{1}H NMR spectrum of L$_3$H$_2$ in CHCl$_3$-*d*$_1$, the deuterium exchangeable protons of the =N—OH groups show only one broad peak, with chemical shifts as singlet at 11.10–11.65 ppm, which indicates an (*E,E*)-configuration for *vic*-dioxime [15]. The chemical shifts that belong to —NH protons were observed at 5.26 ppm as a singlet for L$_1$H$_2$, at 5.08 ppm as a singlet for L$_2$H$_2$, and at 5.07–5.18 ppm as a doublet for L$_3$H$_2$, respectively, and disappeared with D$_2$O exchange. The carbon resonances of oxime groups are found at 155.6 and 149.0 ppm for L$_1$H$_2$ and 143.8 and 148.4 ppm for L$_2$H$_2$, respectively. These nonequivalent carbon atoms, which particularly belong to hydroxyimino carbon atoms, also confirm the *anti* structure for L$_1$H$_2$ and L$_2$H$_2$ [16]. The ^{1}H NMR spectra of the nickel(II) complexes show peaks at $\delta = 15.20$ ppm for [Ni(L$_1$H)$_2$] and at $\delta = 15.65$ ppm for [Ni(L$_2$H)$_2$], supporting the proposed (O—H··O) bridge [5a,17,18]. This result can easily be identified by deuterium exchange. Other NMR spectra of ligands and Ni(II) complexes are given in Table 4.

FT-IR Spectra

The characteristic IR group frequencies data are given in Table 2. The IR spectra of the Ni(II) complexes were interpreted by comparing these spectra with those of the free ligands. In the IR spectrum of ligands, the —OH stretching vibrations were observed at 3090–3671 cm^{-1} for L$_1$H$_2$, 3132–3653 cm^{-1} for L$_2$H$_2$, and 3060–3605 cm^{-1} for L$_3$H$_2$, respectively. The —NH stretching vibrations were observed at around 3284 cm^{-1} for L$_1$H$_2$, 3299 cm^{-1} for L$_2$H$_2$, and 3384 cm^{-1} for L$_3$H$_2$, respectively. The characteristic shift of azomethine (—C=N) peak, from 1636–1656 to 1609–1650 cm^{-1}, indicates the coordination of the azomethine nitrogen to the nickel center. However, the disappearance of —OH stretching peak in the IR spectrum of ligands together with the existence of H-bridge (O—H··O) at near 1730–1769 cm^{-1} as well as the shifting of —C=N and —N—O stretches in the IR spectra of the Ni(II) complexes provide support for MN$_4$ or MN$_4$·2H$_2$O type coordination in the complexes [19]. In the IR spectrum of ligands, strong peaks at 974, 1000, and 1004 cm^{-1} are assignable to N—O stretching vibrations [5a,20].

SCHEME 1 Synthetic route to the *vic*-dioxime ligands (L$_1$H$_2$, L$_2$H$_2$, and L$_3$H$_2$).

TABLE 1 Formula Weight, Color, Melting Point, Yield, Magnetic Susceptibility, and Elemental Analysis of the Ligands and their Complexes

Compounds	Formula Weight (g/mol)	Color	Melting Point (°C)	Yield (%)	μ_{eff} (BM)	Elemental Analyses Calcd. (Found) %		
						C	H	N
Ligand, L_1H_2 $C_{16}H_{22}N_4O_4$	334	Yellow	102	71	–	57.48 (57.02)	6.59 (7.12)	16.76 (16.18)
$[Ni(L_1H)_2]$ $C_{32}H_{42}N_8O_8Ni$	725	Red	214	68	Dia	52.96 (53.14)	5.79 (5.32)	15.45 (14.98)
Ligand, L_2H_2 $C_{10}H_{18}N_4O_4$	258	Light Yellow	103	75	–	46.51 (47.30)	6.98 (7.25)	21.70 (22.06)
$[Ni(L_2H)_2]$ $C_{20}H_{34}N_8O_8Ni$	573	Red	234	72	Dia	41.88 (41.26)	5.93 (5.42)	19.55 (18.98)
Ligand, L_3H_2 $C_{18}H_{32}N_6O_6$	428	Yellow	123	48	–	50.47 (50.13)	7.48 (7.20)	19.63 (19.24)
$[Ni(L_3H)_2 \cdot 2H_2O]$ $C_{36}H_{66}N_{12}O_{14}Ni$	949	Red	168	52	2.93	45.52 (44.97)	6.95 (6.56)	17.70 (17.23)

Dia = diamagnetic.

TABLE 2 Characteristic IR Bands (cm^{-1}) of the Ligands and Complexes as KBr Pellets

Compounds	O—H	N—H	Aliphatic C—H	O-H···O	N—O	C=N	C=O
L_1H_2	3090–3671	3284	2860–2982	–	1000	1639	1675
$[Ni(L_1H)_2]$	–	3299	2846–2984	1769	964	1609	1697
L_2H_2	3132–3653	3299	2859–2935	–	1004	1636	1674
$[Ni(L_2H)_2]$	–	3310	2865–3010	1734	982	1597	1702
L_3H_2	3060–3605	3384	2859–2977	–	974	1656	1697
$[Ni(L_3H)_2 \cdot 2H_2O]$	3048–3611	–	2865–2983	1730	970	1650	1683

TABLE 3 Characteristic UV-Visible Bands of the Ligands and Ni(II) Complexes

Compounds	Solvent	Wavelength [λ_{max} (nm)] (logε)				
L_1H_2	DMSO	224 (6.14)	286 (5.86)	318s (3.92)		
	C_2H_5OH	215 (5.23)	237 (4.46)	275 (3.64)		
$[Ni(L_1H)_2]$	DMSO	259 (5.64)	292 (5.18)	384s (4.21)	547 (3.04)	
	C_2H_5OH	210 (5.86)	259s (4.63)	315 (3.61)	537 (2.34)	
L_2H_2	DMSO	221 (4.41)	270 (3.07)	293 (2.56)		
	C_2H_5OH	248 (5.04)	326 (4.28)	416s (2.30)		
$[Ni(L_2H)_2]$	DMSO	218 (5.06)	264 (4.72)	318 (3.12)	554 (2.10)	567 (1.98)
	C_2H_5OH	213 (4.96)	259 (4.48)	383 (3.57)	483 (3.16)	
L_3H_2	DMSO	226 (5.08)	272 (4.36)	336 (2.18)		
	C_2H_5OH	228 (5.34)	296 (4.73)	348 (3.40)		
$[Ni(L_3H)_2 \cdot 2H_2O]$	DMSO	231 (5.16)	261 (4.56)	326s (3.38)	598 (2.14)	584 (2.16)
	C_2H_5OH	214 (6.04)	272 (4.82)	332s (3.10)	429 (2.93)	

s = shoulder.

TABLE 4 ^1H NMR Spectra of the Ligands and Ni(II) Complexes

Functional Group	L_1H_2 (CHCl$_3$)	$[Ni(L_1H)_2]$ (CDCl$_3$)	L_2H_2 (CHCl$_3$)	$[Ni(L_2H)_2]$ (DMSO)	L_3H_2 (CHCl$_3$)
(O—H···O)[a]	–	15.20 (2H)^s	–	15.65 (2H)^s	–
OH[a]	10.70 (1H)^s	–	8.32 (1H)^s	–	11.10–11.65
	9.56 (1H)^s		8.54 (1H)^s		(2H)[b]
H—C=N	–	–	7.45 (1H)^s	7.76 (2H)^s	–
—NH[a]	5.26 (1H)^s	4.64 (2H)^s	5.08 (1H)^s	5.68 (2H)^s	5.07–5.18 (2H)[d]
O—CH$_2$ and NH—CH	3.80–4.22 (3H)^m	3.72–4.15 (6H)^m	3.86–4.18 (3H)^m	3.82–3.98 (6H)^m	4.06–4.18 (6H)^m
N—CH$_2$	2.52–2.70 (4H)^t	2.50–2.65 (8H)^t	1.80–2.10 and 2.80–3.06 4(H)^t	2.43–2.88 (8H)^m	2.80–2.98 (8H)^m
Ar-CH	7.65–7.80 (2H)^s	7.38 (6H)^s	–	–	–
	7.35–7.45 (3H)^s	7.54 (4H)^s			
C—CH$_3$	1.20–1.45 (3H)^m	1.22–1.26 (6H)^m	1.08–1.29 (7H)^m (for C—CH$_3$ and Cyc—CH$_2$)	1.12–1.98 (14H)^m (for C—CH$_3$ and Cyc—CH$_2$)	1.20–1.35 (6H)^m
Cyc—CH$_2$	0.80–0.98 (4H)^m	1.81–1.84 (8H)^m			1.86–1.98 (2H)^m

m: multiplet, s: singlet, d: doublet, t: triplet, a: deuterium exchangeable, and b: broad peaks.

TABLE 5 Voltammetric parameters of the complexes versus Ag/AgCl (Fc/Fc$^+$) in DMSO-TEAP; values in parenthesis: versus Fc/Fc$^+$

Complexes	M^{2+}/M^{3+} $E_{1/2}{}^a$ (V)	$\Delta E_p{}^b$ (V)	$I_{p,a}/I_{p,c}{}^c$	M^{2+}/M^+ $E_{1/2}{}^a$ (V)	$\Delta E_p{}^b$ (V)	$I_{p,a}/I_{p,c}{}^c$	L/L^- $E_{1/2}{}^a$ (V)	$\Delta E_p{}^b$ (V)	$I_{pa}/I_{pc}{}^c$	L/L^+ $E_{1/2}{}^a$ (V)
[Ni(L$_1$H)$_2$]	0.382 (−0.108)			−0.745 (−1.24)	0.330	0.97	−1.25 (−1.74)	0.090	0.85	0.683 (0.193)
[Ni(L$_2$H)$_2$]	0.392 (−0.098)	0.080	0.95	−0.840	0.320 (−1.33)	0.35	−1.43 (−1.92)	0.130	0.41	0.721 (0.231)
[Ni(L$_3$H)$_2$·2H$_2$O]							−1.18 (−1.67)			0.827 (0.337)

[a]Cathodic peak potential for reduction and anodic peak potential for oxidation for irreversible processes.
[b]$\Delta E_p = E_{p,c} - E_{p,a}$ at 0.100 V s^{-1} scan rate.
[c]$I_{p,a}/I_{p,c}$ for reduction and $I_{p,c}/I_{p,a}$ for oxidation at 0.100 V s^{-1} scan rate.

UV-Visible Spectra

Electronic spectra of nickel(II) complexes with L$_1$H$_2$, L$_2$H$_2$, and L$_3$H$_2$ ligands have been recorded in DMSO and C$_2$H$_5$OH solutions as shown in Table 3. Each ligand and metal complex show several intense absorptions in the visible and ultraviolet region. The absorption peaks of ultraviolet region are assignable to the transitions involving ligands orbitals [21]. In the electronic spectra of the ligands and their metal complexes, a wide range of peaks seems to be due to the $\pi \rightarrow \pi^*$, n $\rightarrow \pi^*$, and d–d transitions of C=N as well as charge-transfer transitions arising from π electron interactions between the metal and ligand, which involves either a metal-to-ligand or a ligand-to-metal electron transfer [22,23]. The peaks observed in the 210–272 nm range can be assigned to the $\pi \rightarrow \pi^*$ transitions of the aromatic rings. The absorption peak observed within the 315–348 nm region for three ligands is most probably due to the transition of n $\rightarrow \pi^*$ of imine groups [24]. The weak d–d transitions of [Ni(L$_1$H)$_2$], [Ni(L$_2$H)$_2$], and [Ni(L$_3$H)$_2$·2H$_2$O] could be observed at 547, 554, and 598 nm in DMSO, respectively, while these transitions are observed at 537 nm for [Ni(L$_1$H)$_2$], 483 and 567 nm for [Ni(L$_2$H)$_2$], and 429 and 584 nm for [Ni(L$_3$H)$_2$·2H$_2$O] in ethanol. These spectral changes observed in different solvents are probably due to structural changes of the complexes in DMSO, which may coordinate to the Ni(II) center.
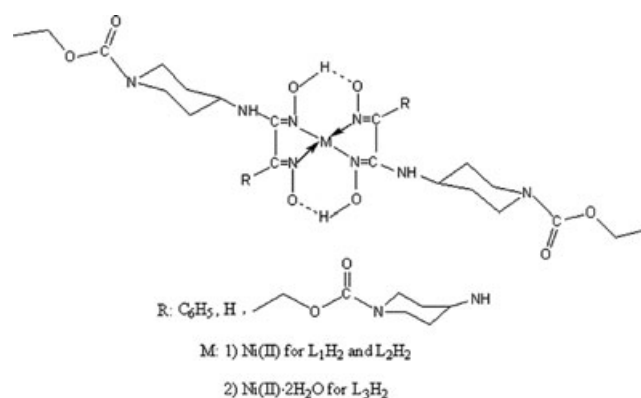
Magnetic Moments

The magnetic moment measurements (Table 1) carried out at room temperature show that [Ni(L$_1$H)$_2$] and [Ni(L$_2$H)$_2$] complexes are diamagnetic, indicating the low spin (S=0) square planar d^8-systems as expected. However, [Ni(L$_3$H)$_2$·2H$_2$O] complex is paramagnetic and its magnetic susceptibility is 2.93 BM. The alternative chemical environment

gives two (O−H··O) bridge protons in the *cis*-form, but only one in the *trans*-form. The observation of the (O−H··O) in the IR and ^{1}H NMR spectra at one frequency in each case indicates that the nickel(II) complex is in the *anti*-form. According to the above results, a square-planar geometry is suggested for the [Ni(L$_1$H)$_2$] and [Ni(L$_2$H)$_2$] complexes [20,25–27] and an octahedral one for the [Ni(L$_3$H)$_2$·2H$_2$O] complex. Structures of the Ni(II) complexes are shown in Fig. 1.

Molar Conductivity

Ni(L$_1$H)$_2$, Ni(L$_2$H)$_2$, and [Ni(L$_3$H)$_2$·2H$_2$O] complexes are nonelectrolytes as shown by their molar conductivity (Λ_M) in 10^{-3} M DMF. Their molar conductivities were found as 2.6 Ω^{-1} cm^2 mol^{-1} for Ni(L$_1$H)$_2$, 3.3 Ω^{-1} cm^2 mol^{-1} for Ni(L$_2$H)$_2$, and 6.3 Ω^{-1} cm^2 mol^{-1} for [Ni(L$_3$H)$_2$·2H$_2$O].

R: C$_6$H$_5$, H ,

M: 1) Ni(II) for L$_1$H$_2$ and L$_2$H$_2$
2) Ni(II)·2H$_2$O for L$_3$H$_2$

FIGURE 1 Mononuclear Ni(II) complexes of L$_1$H$_2$, L$_2$H$_2$, and L$_3$H$_2$ ligands.
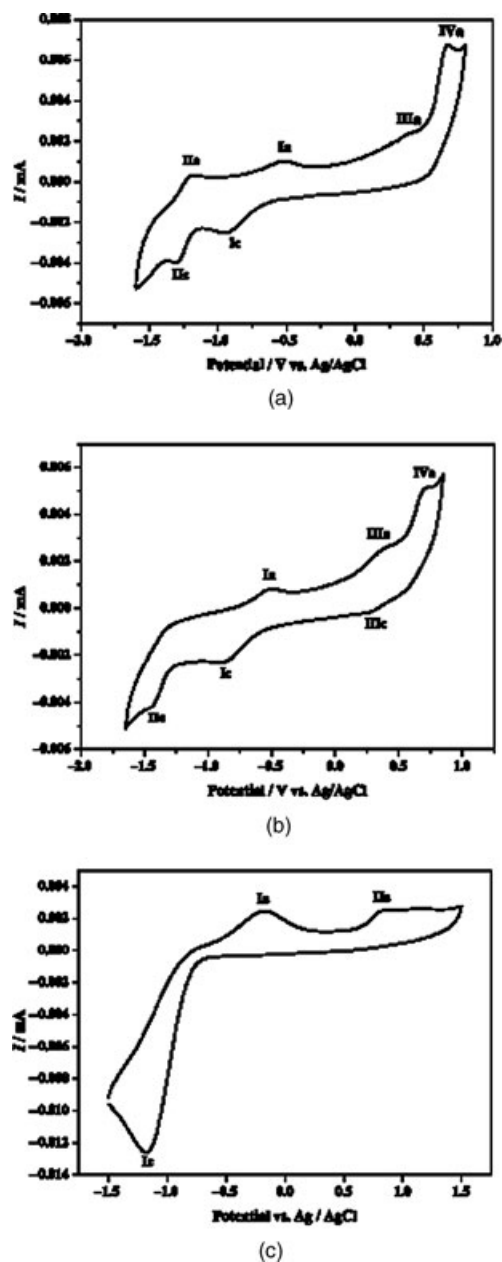
FIGURE 2 Cyclic voltammograms of the nickel complexes in DMSO containing 0.1 M TEAP as supporting electrolyte: (a) for [Ni(L$_1$H)$_2$], (b) for [Ni(L$_2$H)$_2$], and (c) for [Ni(L$_3$H)$_2$·H$_2$O] complexes.

Electrochemistry

The electrochemical properties of the three oxime complexes, [Ni(L$_1$H)$_2$], [Ni(L$_2$H)$_2$], and [Ni(L$_3$H)$_2$·2H$_2$O], coordinate in different environments on the main oxime moiety, were investigated using cyclic voltammetric (CV) technique in DMSO containing an Ag/AgCl electrode system. The data collected in this works are summarized in Table 5. As seen from Fig. 2(a), [Ni(L$_1$H)$_2$] complex displayed

two reduction peaks at −0.745 V and −1.245 V versus Ag/AgCl, with the corresponding anodic waves on the reverse scan. The first and second reduction peaks could be assigned to the Ni(II)/Ni(I) species and oxime moities, respectively. The ligand-based reduction in the oxime complexes could be expected to occur at more negative potentials owing to the polarization of the oxime moities in DMSO. Although the high value for the anodic-to-cathodic peak separation ($\Delta E_p = 0.330$ V) of the first reduction couple at 0.010 V. s^{-1} was found, the anodic-to-cathodic peak current ratio ($I_{p,a}/I_{p,c}$) equal to unity for the first reduction couple at high scan rates indicates quasi-reversible electron transfer mechanism. The anodic-to-cathodic peak separation (ΔE_p) of the second reduction couple was 0.090 V at 0.010 V. s^{-1} and the anodic-to-cathodic peak current ratio ($I_{p,a}/I_{p,c}$) for this couple is equal to unity. This behavior indicates that the second couple has reversible character even at high scan rates. In addition, [Ni(L$_1$H)$_2$] gives an oxidation peak at 0.382 V versus Ag/AgCl without the corresponding cathodic wave even at very high scan rates. This peak can be attributed to Ni(II)/Ni(III) monocationic species. The absence of the cathodic signal indicates a fast chemical reaction following the charge-transfer step and instability of electrochemically generated nickel(III) species. It is well known that the oxidation or reduction processes of metal ions occur usually prior to the oxime moities in metal-oxime complexes [28–30]. [Ni(L$_1$H)$_2$] also displayed an irreversible ligand oxidation peak at 0.683 V versus Ag/AgCl with the low value of the ratio of the cathodic current-to-anodic current on the reverse scan and the anodic-to-cathodic peak separation ($\Delta E_p = 0.140$ V). But it is unusual to observe the ligand-based oxidation process within the available solvent potential window. The CV of [Ni(L$_2$H)$_2$] complex is shown in the Fig. 2(b), which indicates two reduction and two oxidation peaks corresponding to reoxidation and rereduction waves on the scan rate. In the nickel-oxime complex series, only [Ni(L$_2$H)$_2$] gave reversible oxidation process based on the metal ion with a convenient peak separation ($\Delta E_p = 0.080$ V) and the ratio of the anodic peak current-to-cathodic peak current equal to unity. The electrogenerated species during the first oxidation process are assignable to Ni(II)/Ni(III) couples, the half-wave potential of which is located at 0.392 V versus Ag/AgCl. The first reduction process also assigns to metal-based reduced Ni(II)/Ni(I) species, which exhibits irreversible character at different scan rates due to the instability of the electrogenerated Ni(II)/Ni(I) species. The cathodic and anodic peak potentials for the ligand-based reduction and oxidation processes are located at −1.43 V

and 0.721 V, respectively, the former of which shows the most negative shift in the metal-oxime complex series studied in this work. The electrochemistry of [Ni(L$_3$H)$_2$·2H$_2$O] complex exhibited considerably different behavior in the complex series. As could be seen from Fig. 2(c), the complex displayed only one reduction and one oxidation couples at −1.18 V and 0.827 V versus Ag/AgCl, respectively. The oxidation step exhibits totally irreversible anodic wave without corresponding cathodic wave even at very high scan rates. The absence of the cathodic peak could be attributed to a fast chemical reaction following the charge-transfer step and causes instability of monoanionic species. The reduction has a large peak separation, which indicates totally irreversible character for the electron transfer reaction. The reduction and oxidation processes assign to the oxime moity, the former of which shows an adsorption peak while a usual diffusion-controlled process occurs for the latter [31]. Direct proportionality of the cathodic peak current with the scan rate provides evidence for the adsorption character of reduction wave [31]. The anodic or cathodic peak potentials of the complexes could be expected to shift by the introduction of electron-donating or electron-withdrawing groups on the oxime moity as previously observed for phthlocyanine complexes [32–36]. However, the experimental results showed that no introduction of the electron-donating phenyl groups on the oxime moity for [Ni(L$_2$H)$_2$] complex provided shift as expected. But the adsorption and the absence of oxidation and reduction waves based on the metal center for the [Ni(L$_3$H)$_2$·2H$_2$O] complex are the main differences compared with the electrochemistry of the [Ni(L$_1$H)$_2$] and [Ni(L$_2$H)$_2$] complexes in the same experimental condition. These behaviors could be attributed to the highly polarized [Ni(L$_3$H)$_2$·2H$_2$O] complex that has four carboxylate groups attached to piperidine on the oxime moieties.

REFERENCES

[1] Tschugaeff, L. Chem Ber 1905, 38, 2520.
[2] Chugaev,L. A. Zh Russ Physicochem Soc 1909, 41, 184.
[3] (a) Smith, P. A. The Chemistry of Open-Chain Organic Nitrogen Compounds; WA Benjamin: New York, 1966; Vol. 2.; (b) Gök, Y.; Kantekin, H. New J Chem 1995, 19, 461.
[4] Brown, B. G. Prog Inorg Chem 1973, 18, 17.
[5] (a) Ahsen, V.; Bekaroglu, O. Synth React Inorg Met-Org Chem 1985, 15, 61; (b) Ahsen, V.; Gokceli, F.; Bekaroglu, O. J Chem Soc Dalton Trans 1987, 1827; (c) Musluoğlu, E.; Ahsen, V. J Chem Res (S) 1999, 142.
[6] Nesmeyanow, A. N.; Nesmeyanow, N. A. Fundamentals of Organic Chemistry, 2nd ed., English translation, Mir Publishers: Moscow, 1981; Vol. 3, p. 167.
[7] Ploty, O.; Steinbock, H. Chem Ber 1902, 35, 3113.
[8] Britzingen, H.; Titzmann, R. Ber Dtsch Chem Ges 195, 85, 345.
[9] Panzio, G.; Baldracco, F. Gazz Chim ›taly 1930, 60, 415.
[10] Earnshaw, A. Introduction to Magnetochemistry; Academic Press: London, 1968; p. 4.
[11] Brand, U.; Vahrenkamp, H. Chem Ber 1996, 129, 435.
[12] Zhang, Z.; Martell, A. E.; Motekaitis, R.T.; Fu, L. Tetrahedron Lett 1999, 40, 4615.
[13] Gül, A.; Bekaroğlu, Ö. J Chem Soc Dalton Trans 1983, 2537.
[14] Sevindir, H. C. Synth React Inorg Met-Org Chem 1996, 26(4), 605.
[15] Durmus, M.; Ahsen, V.; Luneau, D.; Pecaut, J. Inorg Chim Acta 2004, 357, 588.
[16] Gök, Y.; Kantekin, H.; Alp, H.; Özdemir, M. Z Anorg Allg Chem 1995, 621, 1237.
[17] Tas, E.; Cukurovali, A. J Coord Chem 1999, 47, 425.
[18] Tas, E.; Aslanoglu, M.; Kilic, A.; Kara, Z. Trans Met Chem 2005, 30, 758.
[19] Kandaz, M.; Koca, A.; Özkaya, A. R. Polyhedron 2004, 23, 1987.
[20] Tas, E.; Aslanoglu, M.; Kilic, A.; Ulusoy, M.; Guler, M. Polish J Chem 2005, 79, 1739.
[21] Das, A. K.; Peng, S. M.; Bhattacharya, S. Polyhedron, 2001, 20, 327.
[22] Sacconi, L.; Ciampolini, M.; Maffio, F.; Cavasino, F. P. J Am Chem Soc 1962, 84, 3245.
[23] Carlin, R. L. Transition Metal Chemistry; Marcel Dekker: New York, 1965; Vol. 1.
[24] Fraser, C.; Bosnich, B. Inorg Chem 1994, 33, 338.
[25] Verani, C. N.; Bill, E.; Renchler, E.; Weyhermuller, T.; Chaudhuri, P. J Chem Soc Dalton Trans 2000, 4263.
[26] Gok, Y.; Ozcan, E. Trans Met Chem 1985, 16, 393.
[27] Cotton, F. A.; Wilkinson, G. Advanced Inorganic Chemistry, 5th ed.; Wiley-Interscience Publication, 1988; p. 725.
[28] Kandaz, M.; Yilmaz, I.; Keskin, S.; Koca, A. Polyhedron 2002, 21, 825.
[29] Kandaz, M.; Coruhlu, S. Z.; Yilmaz, I.; Ozkaya, A. R. Trans Met Chem 2002, 27, 877.
[30] Yilmaz, I.; Kandaz, M.; Özkaya, A. R.; Koca, A. Monatshefte für Chemie 2002, 133, 609.
[31] Bard, A. J.; Faulkner, L. R. (Eds.). Electrochemical Methods: Fundamentals and Applications, 2nd ed.; Wiley: New York, 2001; p. 228.
[32] Kadish, K. M.; Nakanishi, T.; Gürek, A. G.; Ahsen, V.; Yilmaz, I. J Phy Chem B 2001, 105, 9817.
[33] Yilmaz, I.; Nakanishi, T.; Gürek, A. G.; Kadish, K. M. J Porphyrins Phthalocyanines 2003, 7, 227.
[34] Nakanishi, T.; Yilmaz, I.; Nakashima, N.; Kadish, K. M. J Phys Chem B 2003, 107, 12789.
[35] Yilmaz, I.; Kocak, M. Polyhedron 2004, 23, 1279.
[36] Yilmaz, I.; Gurek, A. G.; Ahsen, V. Polyhedron 2005, 24, 791.